J. theor. Biol. (1998) **193,** 577–592
Article No. jt980723

Networks with Side Branching in Biology

D. L. TURCOTTE*, J. D. PELLETIER* AND W. I. NEWMAN†

* *Department of Geological Sciences, Cornell University, Ithaca, NY* 14853, *U.S.A.* and
† *Department of Earth and Space Sciences, Physics and Astronomy, and Mathematics, University of California, Los Angeles, CA* 90095, *U.S.A.*

(*Received on* 10 *November* 1997, *Accepted in revised form on* 13 *April* 1998)

There are many examples of branching networks in biology. Examples include the structure of plants and trees as well as cardiovascular and bronchial systems. In many cases these networks are self-similar and exhibit fractal scaling. In this paper we introduce the Tokunaga taxonomy for the side branching of networks and his parameterization of self-similar side-branching. We introduce several examples of deterministic branching networks and show that constructions with the same fractal dimension can have different side-branching parameters. As an example of stochastic-branching in biology we consider the vein structure of a leaf. We show that the vein structure of the leaf and river networks have nearly identical side branching statistics. We introduce diffusion limited aggregation (DLA) clusters. These clusters also exhibit Tokunaga side-branching statistics. We consider several alternative explanations for why leaves, river networks, and DLA clusters have similar side-branching statistics. We also consider the allometric scaling relation between metabolic rate and the mass of species in terms of a cardiovascular system with Tokunaga statistics. We find reasonably good agreement between the observed scaling exponent, ≈ 0.75, and our model for a range of values of the fractal dimension of the network and the blood flow resistance parameter.

1. Introduction

Simple branching networks are most easily illustrated by river networks. The merging of small streams gives larger streams, large streams merge to give small rivers, and so forth. But small streams can also merge with larger streams and rivers. The branching statistics of networks can differentiate between alternative models for their formation. The original taxonomy for branching networks was given by Horton (1945). Strahler (1957) introduced a slightly modified system which is now widely used in a variety of applications. In this classification system a stream with no upstream tributaries is defined to be a first order ($i = 1$) stream. When two-first order streams combine they form a second-order ($i = 2$) stream, when two second-order streams combine they form a third-order ($i = 3$) stream, and so forth. The total number of i-th order streams is N_i and their mean length L_i.

Horton (1945) defined the branching ratio R_N according to

$$R_N = \frac{N_i}{N_{i+1}} \tag{1}$$

and also introduced the length-order ratio

$$R_L = \frac{L_{i+1}}{L_i} \tag{2}$$

Empirically it was recognized that both R_N and R_L are nearly constant for a range of stream orders for all river networks and this observation constitutes two of Horton's laws.

As Mandelbrot (1982) developed fractal concepts he recognized that Horton's laws define a fractal tree.

0022–5193/98/160577 + 16 $30.00/0

The fractal dimension D for a river network can be expressed in terms of the branching and length-order ratios according to

$$D = \frac{\log R_N}{\log R_L} \tag{3}$$

Thus the validity of Horton's laws implies that drainage networks are fractal trees. Fractal scaling implies scale invariance.

The Horton–Strahler taxonomy has been applied widely in biology. Examples include trees (Leopold, 1971; Barker *et al*., 1977; Zeide & Gresham, 1991), leaves (Fisher & Honda, 1979), bronchial systems (Horsfield *et al*., 1971; Horsfield, 1980, 1990; Nelson *et al*., 1990) and cardiovascular systems (MacDonald, 1983; West, 1990; Bassingthwaighte *et al*., 1994; Li, 1996). Many of these applications satisfy the fractal relation (3) to a good approximation.

A major improvement in the quantitative classification of self-similar networks was introduced by Tokunaga (1978, 1984, 1994). In the Tokunaga taxonomy the details of side branching are considered. Self-similar trees that have identical Horton–Strahler taxonomies can have very different Tokunaga taxonomies. The Tokunaga approach has been applied to drainage networks (Peckham, 1995) but has not been used in biological applications.

In this paper we first introduce the Tokunaga taxonomy and give several deterministic examples. The Tokunaga classification approach was independently developed for diffusion limited aggregation (DLA) clusters (Vannimenus & Viennot, 1989) and this application is discussed. We next compare the vein structure of a leaf with a river network. We suggest that DLA growth is responsible for the structure of both river networks and leafs. And finally we consider allometry with a particular application to the dependence of the metabolic rate of species on their mass. We extend the considerations of allometry given by West *et al*. (1997) to Tokunaga taxonomies.

2. The Tokunaga Taxonomy

A small example of a river network is given in Fig. 1(a). The 100 m scale is shown, without the specified scale it would be impossible to tell whether the drainage network covered 1 or 1000 km. An example of a binary deterministic fractal tree is given in Fig. 1(b). This is a highly ordered structure in which the single third-order ($i = 3$) stem bifurcates into two second-order ($i = 2$) branches each with one-half the length of the stem, these two second-order branches in turn bifurcate to form four first-order ($i = 1$) branches each of one-quarter the length of the stem. Obviously this construction could be carried to higher and higher orders.

However, a major difference between this binary tree and the river network is the absence of side branching. A branch of order n can have any number of side branches of order $n-1$, $n-2, \ldots,$ 1. A fractal tree with side-branching is given in Fig. 1(c). The third-order branch has three side branches, two first order and one second order. Each of the second-order branches has a first-order side branch. In order to classify side branching Tokunaga (1978, 1984, 1994) extended the Strahler ordering system. A first-order branch joining another first-order branch is denoted "11" and the number of such branches is

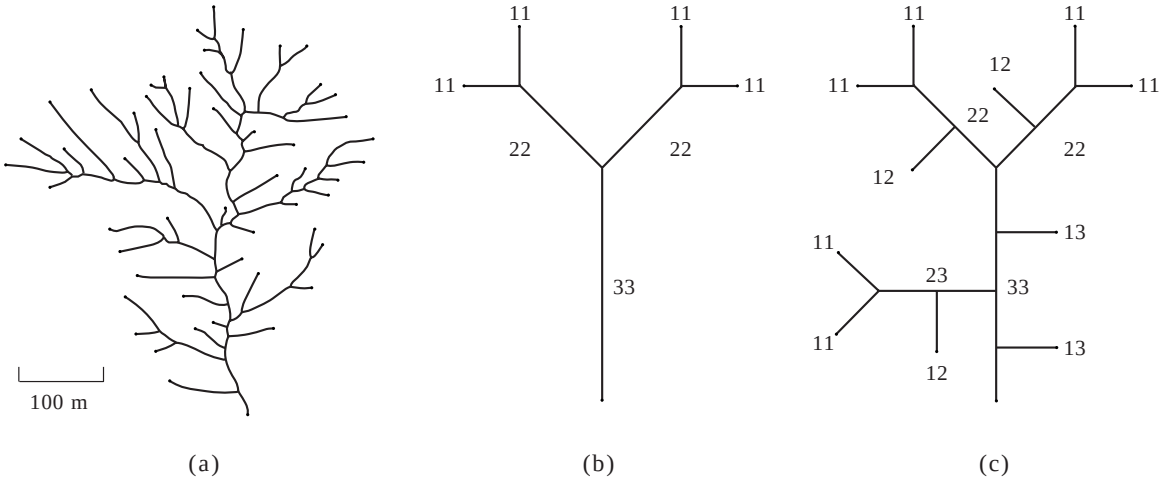

FIG. 1. (a) Example of an actual fourth-order river network; (b) deterministic third-order, binary fractal tree. The third-order stem bifurcates into two second-order branches, the second-order branches bifurcate into two first-order branches; (c) side branches have been added to the binary tree in (b). The third-order branch has two first-order side branches and one second-order side branch. Each second-order branch has a first-order side branch. The Tokunaga ordering system is given.

N_{11}	N_{12}	N_{13}	N_{14}	N_1	20	16	8	7	51	4	0	0	4	6	3	2	11
	N_{22}	N_{23}	N_{24}	N_2		4	3	3	10		2	0	2		2	1	3
		N_{33}	N_{34}	N_3			2	0	2			1	1			1	1
			N_{44}	N_4				1	1								
(a)					(b)					(c)				(d)			

FIG. 2. (a) Illustration of the branching-number matrix, N_{ij} is the number of branches of order i joining branches of order j, N_i is the total number of branches of order i; (b)–(d) branching-number matrices for the fractal trees illustrated in Fig. 1(a)–(c).

N_{11}, a first-order branch joining a second-order branch is denoted "12" and the number of such branches is N_{12}, a second-order branch joining a second-order branch is denoted "22" and the number of such branches is N_{22}, and so forth. This classification of branches is illustrated in Fig. 1.

The branch numbers N_{ij}, $i \leqslant j$, constitute a square, upper-triangular matrix. This formulation is illustrated in Fig. 2(a), the branch-number matrices for the drainage network and deterministic fractals illustrated in Fig. 1(a–c) are given in Fig. 2(b–d). The total number of streams of order i, N_i, is related to the N_{ij} by

$$N_i = \sum_{j=i}^{n} N_{ij} \tag{4}$$

for a fractal tree of order n as illustrated in Fig. 2. The deterministic fractal tree illustrated in Fig. 1(b) has $R_N = 2$ and $R_L = 2$ so that $D = 1$ from (3). The deterministic fractal illustrated in Fig. 1(c) has $R_L = 2$ but R_N is not constant. However, it can be shown that $R_N \to 4$ for large i. Thus from (3)$D \to 2$ for large i.

When considering self-similar (fractal) trees it is convenient to introduce branching ratios T_{ii}, these are the average number of branches of order i joining each branch of order j, $i < j$. Branching ratios are related to branch numbers by

$$T_{ij} = \frac{N_{ij}}{N_j} \tag{5}$$

Again the branching ratios T_{ij} constitute a square, upper-triangular matrix as illustrated in Fig. 3(a). The branching-ratio matrices for the drainage network and deterministic fractals illustrated in Fig. 1(a–c) are given in Fig. 3(b–d).

T_{12}	T_{13}	T_{14}	1.6	4	7	0	0	1	2
	T_{23}	T_{24}		1.5	3		0		1
		T_{34}			0				
(a)				(b)			(c)			(d)													

FIG. 3. (a) Illustration of the branching-ratio matrix, T_{ij} is the average number of branches of order i joining each branch of order j; (b)–(d) branching-ratio matrices for the fractal trees illustrated in Fig. 1(a)–(c).

Self-similarity (fractality) requires that $T_{i,i+k} = T_k$ where T_k is a branching ratio that depends only on $k = j - i$. It is seen from Fig. 3(d) that the deterministic side branching network illustrated in Fig. 1(c) satisfies this condition with $T_{12} = T_{23} = T_1 = 1$, the condition is also satisfied if the construction is extended to higher orders. A general requirement for self-similarity is (Tokunaga, 1978, 1984)

$$T_k = ac^{k-1} \tag{6}$$

This is now a two parameter family of trees and we will define fractal trees in this class to be Tokunaga trees. For the fractal tree illustrated in Fig. 1(c) we have a $a = 1$ and $c = 2$.

The quantities R_N, a, and c are not independent. Assuming a binary Tokunaga tree with side branching we can obtain a relation between them, combining (4), (5), and (6) we write

$$N_i = 2N_{i+1} + \sum_{j=i+1}^{n} N_{ij} = 2N_{i+1} + \sum_{j=i+1}^{n} T_{ij}N_j$$

$$= 2N_{i+1} + \sum_{k=1}^{n-i} T_k N_{i+k} = 2N_{i+1} + a\sum_{k=1}^{n-i} c^{k-1}N_{i+k} \tag{7}$$

If we divide (7) by N_i and introduce the branching ratio from (2) we obtain

$$1 = \frac{2}{R_N} + a\sum_{k=1}^{n-i} \frac{c^{k-1}}{R_N^k} \tag{8}$$

which can be written as

$$1 = \frac{2}{R_N} + \frac{a}{R_N}\left[1 + \left(\frac{c}{R_N}\right) + \cdots + \left(\frac{c}{R_N}\right)^{n-i-1}\right] \tag{9}$$

And if $n - i - 1$ is large we can approximate (9) with

$$1 = \frac{2}{R_N} + \frac{(a/R_N)}{[1 - (c/R_N)]} \tag{10}$$

which becomes the quadratic

$$R_N^2 - (2 + c + a)R_N + 2c = 0 \tag{11}$$

with the solution

$$R_N = \tfrac{1}{2}\{2 + a + c + [(2 + a + c)^2 - 8c]^{1/2}\} \tag{12}$$

For high order, n large, Tokunaga trees that satisfy (6), the branching ratio R_N is obtained from the parameters a and c using (12). For the tree illustrated in Fig. 1(c) with $a = 1$ and $c = 2$ we have $R_N \to 4$ as $n \to \infty$ from (12).

3. Deterministic Area and Volume Filling Fractal Trees

We will now consider a sequence of deterministic fractal trees that are either area-filling ($D = 2$) or

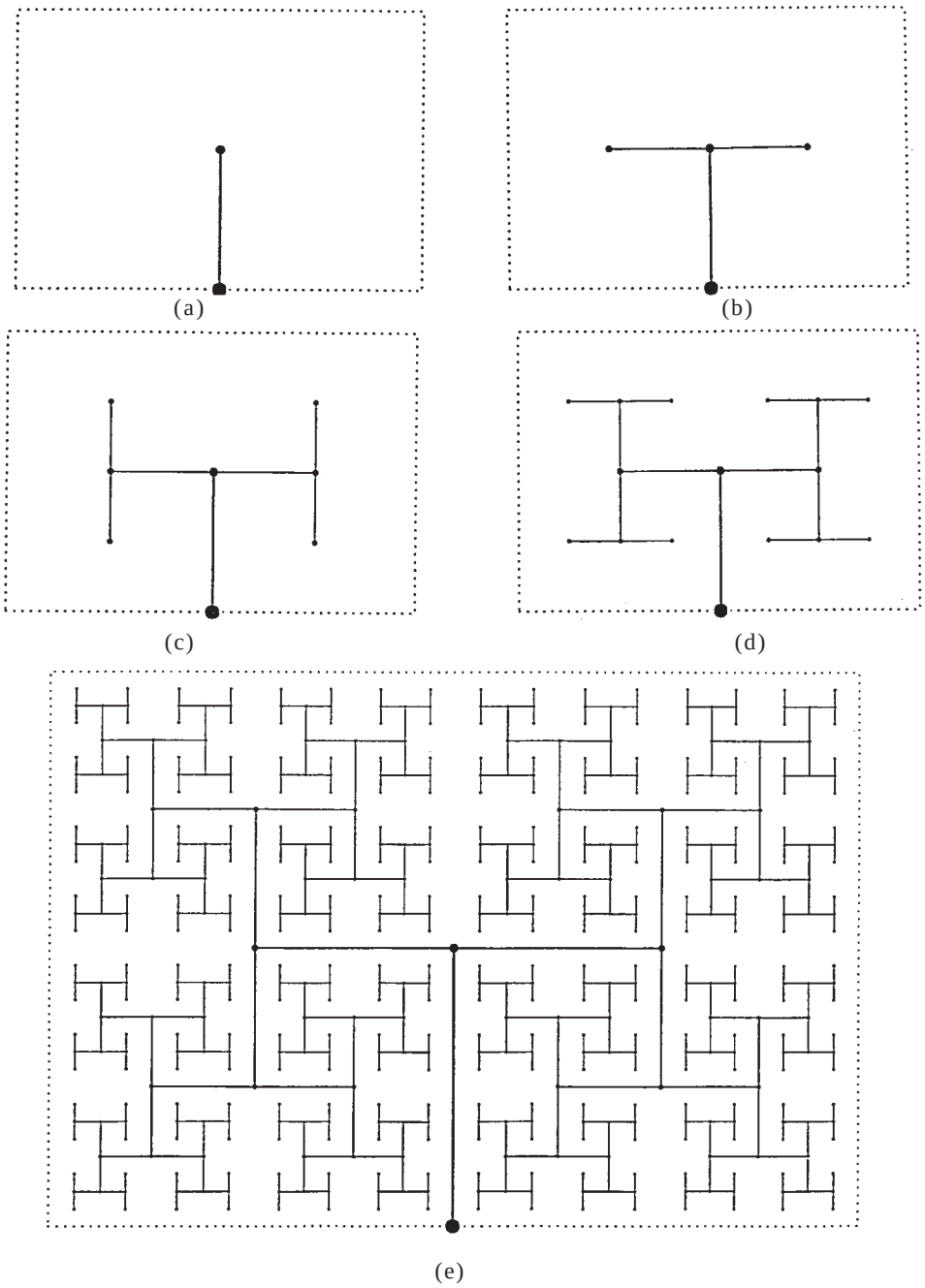

FIG. 4. Deterministic binary fractal tree. With $R_N = 2$ and $R_L = 2^{1/2}$ we have $D = 2$, the construction is area filling without overlap. (a) First-order example; (b) second-order example; (c) third-order example; (d) fourth-order example; (e) ninth-order example.

volume-filling ($D = 3$). We will consider trees with and without side branching and will begin with examples of area-filling trees. A deterministic space-filling fractal tree without side branching is illustrated in Fig. 4. The construction is given at first, second, third, fourth, and ninth orders. A tip node (bud) is placed at the tip of the first-order branch in Fig. 4(a). Two tip branches emanate from this tip node as illustrated in Fig. 4(b). This simple construction is extended to higher and higher orders. The construction given in Fig. 4(b) is the generator for the higher-order trees. For this binary tree we have $R_N = 2$ and $R_L = 2^{1/2}$ so that $D = 2$. When carried to infinite order this fractal tree fills the rectangular region of unit height and width $2^{1/2}$ without overlap.

A deterministic area-filling tree with side branching is illustrated in Fig. 5. The construction is given at first, second, third, and fifth orders. A node (bud) is placed at the tip of the first order

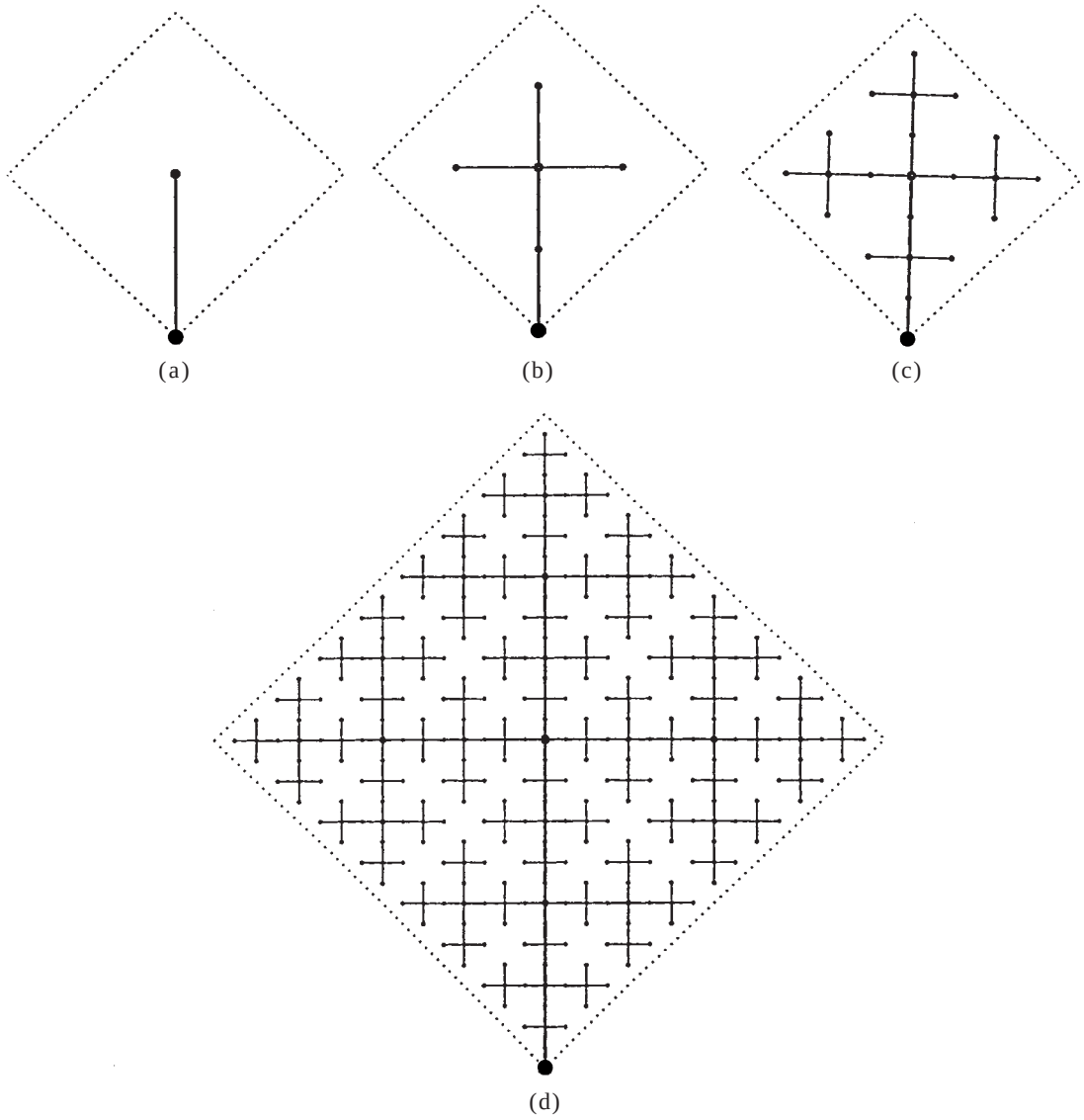

FIG. 5. Deterministic ternary fractal tree with side branching based on a square. With $R_L = 2$ this construction is area filling. (a) First-order example; (b) second-order example, three tip branches emanate from the tip node at first order; (c) third-order example, three tip branches emanate from each tip node and two side branches emanate from the internal node; (d) the construction is extended to fifth order.

$N_{11} = 129$ $N_{12} = 0$ $N_{13} = 22$ $N_{14} = 12$ $N_{15} = 8$
$N_{22} = 33$ $N_{23} = 0$ $N_{24} = 6$ $N_{25} = 4$
$N_{33} = 9$ $N_{34} = 0$ $N_{35} = 2$
$N_{44} = 3$ $N_{45} = 0$
$N_{55} = 1$

(a)

$N_1 = 171$ $R_{N12} = 3.98$ $T_{12} = 0$ $T_{13} = 2$ $T_{14} = 4$ $T_{15} = 8$
$N_2 = 43$ $R_{N23} = 3.91$ $T_{23} = 0$ $T_{24} = 2$ $T_{25} = 4$
$N_3 = 11$ $R_{N34} = 3.67$ $T_{34} = 0$ $T_{35} = 2$
$N_4 = 3$ $R_{N45} = 3.00$ $T_{45} = 0$
$N_5 = 1$

(b) (c)

FIG. 6. (a) Branching-number matrix for the Tokunaga tree illustrated in Fig. 5; (b) numbers of branches of order i, N_i, and bifurcation ratios R_b, the branching ratio approaches 4 ($D \to 2$) for high orders; (c) branching-ratio matrix for the tree.

branch in Fig. 5(a). Three tip branches emanate from this tip node as illustrated in Fig. 5(b). Three tip nodes are placed at the tips of the three tip branches and an interior node bisects the interior branch. Nine tip branches emanate from the three tip nodes and two branches emanate from the internal node as illustrated in Fig. 5(c). Eleven tip nodes are placed at the tips of the 11 external branches and five interior nodes bisect the five interior branches. The construction can be extended to higher and higher order. The length-order ratio for this construction is $R_L = 2$. The branching-number and branching-ratio matrices for the fifth-order construction are given in Fig. 6(a) and (c). The branching ratios for arbitrary order are given by

$$T_k = \begin{cases} 0 & k = 1 \\ 2^{k-1} & k = 2, 3, \ldots \end{cases} \tag{13}$$

The construction is a Tokunaga fractal tree. The branching numbers and bifurcation ratios are given in Fig. 6(b). For large-order trees R_N becomes independent of order and $R_N \to 4$; thus $D \to 2$ and the construction becomes space filling.

Space-filling fractal trees can also be constructed in three dimensions. A binary example with no side branching is illustrated in Fig. 7. The construction is given at first, second, third, fourth, and eighth orders. For this construction we have $R_N = 2$ and $R_L = 2^{1/3}$ so that $D = 3$. When extended to infinite order this construction becomes completely volume filling without overlap. The construction illustrated in Fig. 7 is the three-dimensional analog to the two-dimensional construction illustrated in Fig. 4.

We next illustrate a deterministic volume-filling fractal tree with side branching. The first three iterations are illustrated in Fig. 8. Again a node is placed at the tip of the first-order branch in Fig. 8(a). Seven tip branches emanate from this tip node as illustrated in Fig. 8(b). This construction is based on a hierarchy of body-centered cubic lattices. Seven tip nodes are placed at the tips of the seven tip branches and an interior node bisects the interior branch. Forty-nine tip branches emanate from the seven tip nodes and six branches emanate from the interior node, as illustrated in Fig. 8(c). Again, the construction can be extended to higher and higher order. The length-order ratio for the third-order construction is $R_L = 2$. The branching-number and branching-ratio matrices for this construction are given in Fig. 9(a) and (c). The branching ratios for arbitrary order are given by

$$T_k = \begin{cases} 0 & k = 1 \\ 6 \times 2^{k-2} & k = 2, 3, 4, \ldots \end{cases} \tag{14}$$

Again the construction is a Tokunaga fractal tree. The branching numbers and bifurcation ratios are given in Fig. 9(b). For large-order trees $R_N \to 8$ so that $D \to 3$, the construction becomes volume filling.

The constructions given above show that the Tokunaga taxonomy can differentiate between deterministic constructions that have the same fractal dimension. This has been illustrated in detail by Newman *et al*. (1997). In terms of applications the derived Tokunaga statistics for self-similar fractal networks can distinguish between alternative mechanisms for their generation.

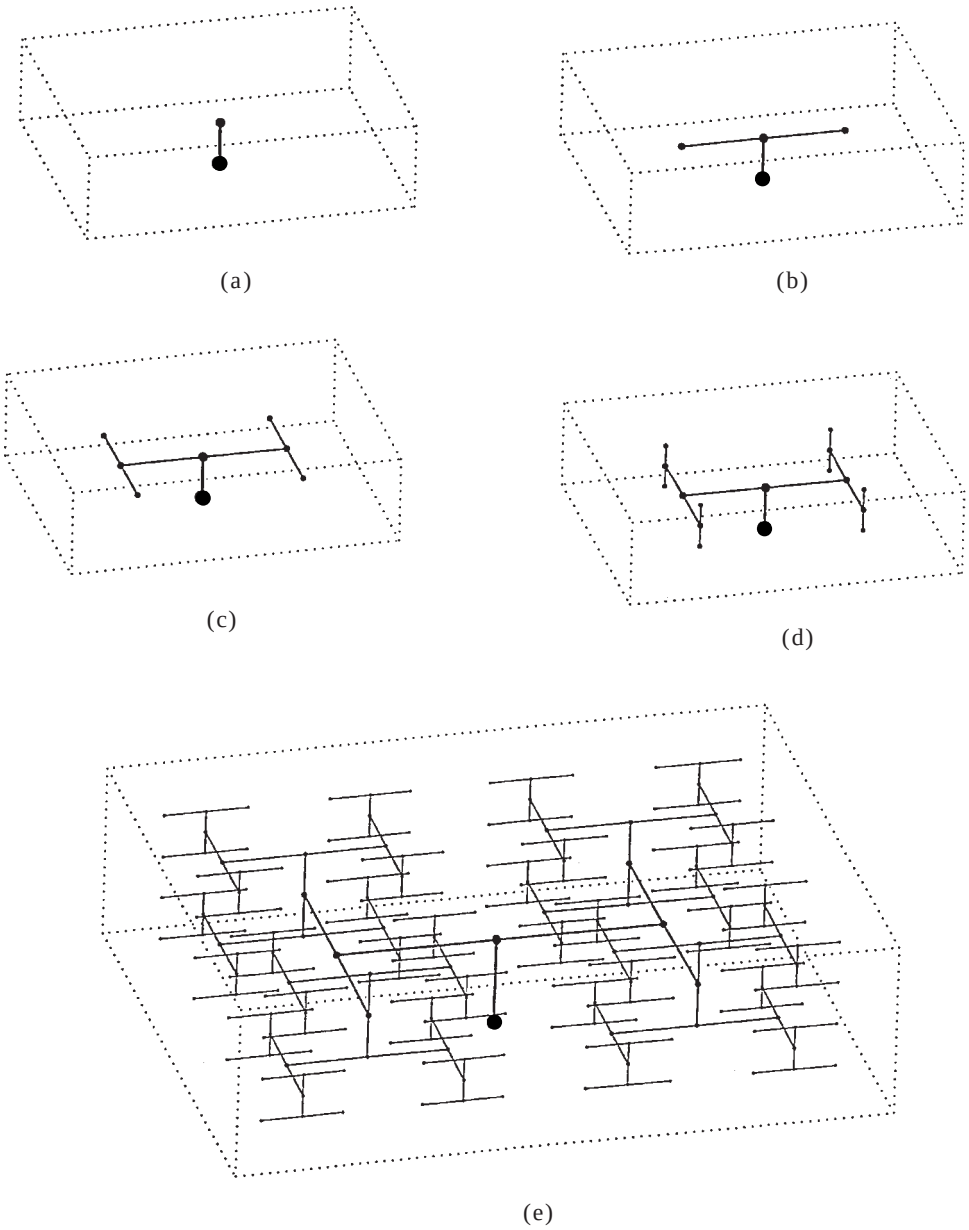

FIG. 7. Three-dimensional binary fractal tree. With $R_N = 2$ and $R_L = 2^{1/3}$ we have $D = 3$, the construction is volume filling without overlap. (a) First-order example; (b) second-order example; (c) third-order example; (d) fourth-order example; (e) eighth-order example.

4. Diffusion Limited Aggregation

A statistical model that generates Tokunaga self-similar fractal networks is diffusion limited aggregation (DLA) introduced by Witten & Sander (1981). They considered a grid of points on a two-dimensional lattice and placed a seed particle near the center of the grid. An accreting particle was randomly introduced on a "launching" circle and was allowed to follow a random path until: (i) it accreted to the growing cluster of particles by entering a grid point adjacent to the cluster or (ii) until it wandered across a larger "killing" circle. A variety of modifications on this simple model have been proposed.

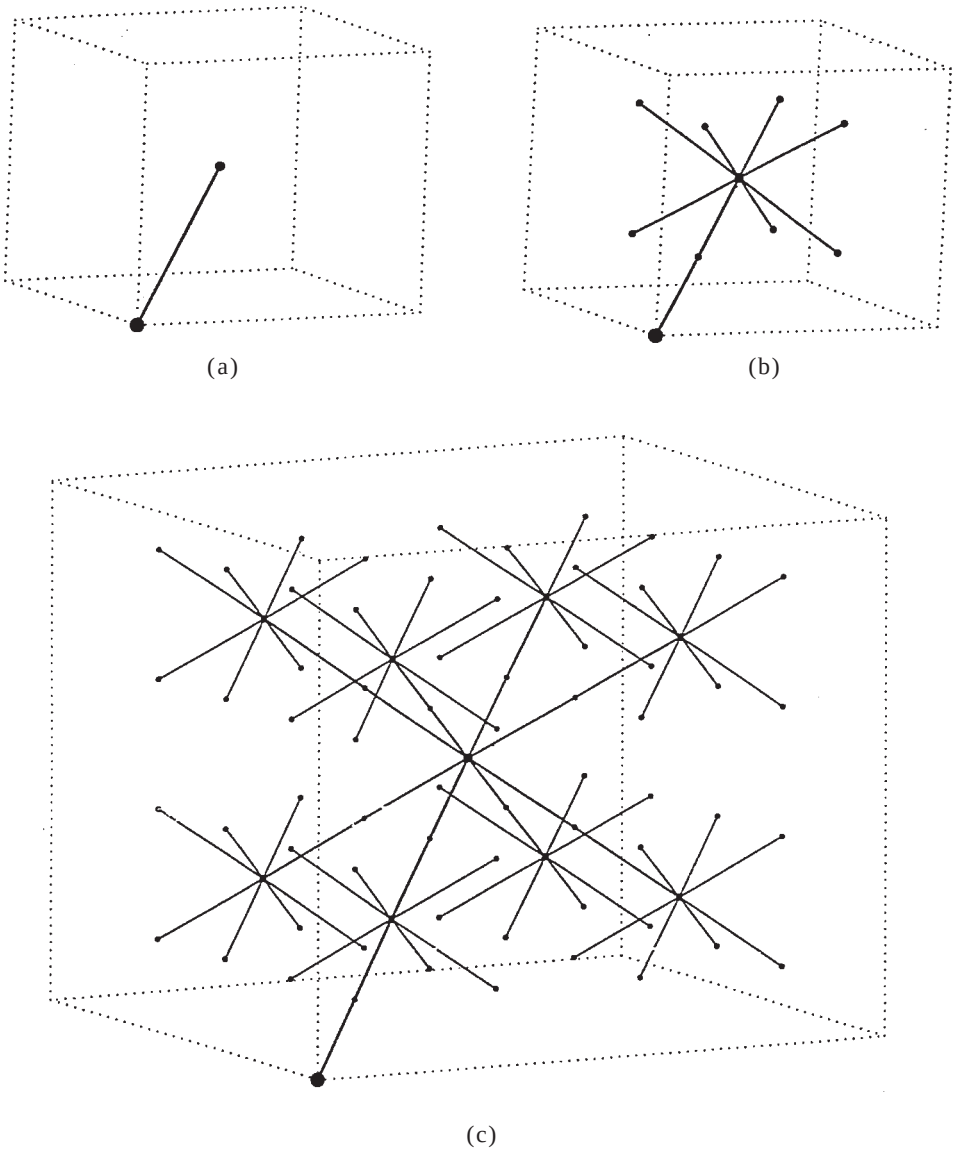

FIG. 8. Deterministic volume filling fractal tree with side branching and $R_L = 2$. The construction is based on a body-centered cubic lattice. Tip nodes emit seven branches at each order and internal nodes emit six branches. (a) First-order example; (b) second-order example; (c) third-order example.

Ossadnik (1992) has considered the side-branching statistics of 47 off-lattice DLA clusters each with 10^6 particles, a typical example is illustrated in Fig. 10. On average the networks were 11-th order fractal trees. The average bifurcation ratio of the clusters was found to $R_N = 5.15 \pm 0.05$ and the average length-order ratio $R_L = 2.86 \pm 0.05$, from (3) the corresponding fractal dimension is $D = 1.56$. In order to analyse the side-branching statistics of DLA clusters Ossadnik (1992) utilized the ramification matrix introduced for DLA by Vannimenus & Viennot (1989). The ramification matrix is entirely equivalent to the branching-ratio matrix introduced by Tokunaga (1978, 1984). In terms of the branching ratios T_{ij}; the terms of the ramification matrix are defined by

$$R_{ij} = \frac{T_{ij}}{\Sigma_{i,i>j} T_{ij}} \tag{15}$$

The terms of the ramification-matrix obtained for DLA by Ossadnik (1992) are given in Fig. 11. For a Tokunaga self-similar fractal tree for which (6) is

$N_{11} = 3073$	$N_{12} = 0$	$N_{13} = 330$	$N_{14} = 84$	$N_{15} = 24$
	$N_{22} = 385$	$N_{23} = 0$	$N_{24} = 42$	$N_{25} = 12$
		$N_{33} = 49$	$N_{34} = 0$	$N_{35} = 6$
			$N_{44} = 7$	$N_{45} = 0$
				$N_{55} = 1$

(a)

$N_1 = 3511$	$R_{N12} = 8.00$	$T_{12} = 0$	$T_{13} = 6$	$T_{14} = 12$	$T_{15} = 24$
$N_2 = 439$	$R_{N23} = 7.98$		$T_{23} = 0$	$T_{24} = 6$	$T_{25} = 12$
$N_3 = 55$	$R_{N34} = 7.87$			$T_{34} = 0$	$T_{35} = 6$
$N_4 = 7$	$R_{N45} = 7$				$T_{45} = 0$
$N_5 = 1$					

(b) (c)

FIG. 9. (a) Branching-number matrix for the Tokunaga tree illustrated in Fig. 8; (b) number of branches of order i, and bifurcation ratios. R_b, the bifurcation ratio approaches 8 ($D \to 3$) for high orders; (c) branching-ratio matrix for the tree.

valid, the terms of the ramification matrix are given by

$$R_{ij} = \frac{T_{j-i}}{\Sigma_{i,i<j} T_{j-i}} = \frac{c^{j-i-1}}{\Sigma_{i,i<j} c^{j-i-1}} \tag{16}$$

For large values of j this becomes

$$R_{ij} = \frac{1}{c^{i-1}}\left(1 - \frac{1}{c}\right). \tag{17}$$

Taking $c = 2.7$ this relation is compared with the DLA data given in Fig. 11. It is seen that DLA clusters are Tokunaga self-similar fractal trees to a good approximation. With $R_N = 5.15$ and $c = 2.7$ we find from (11) that $a = 1.5$.

DLA has a wide variety of applications to natural phenomena (Meakin, 1987, 1991). Examples include dendritic structures in mineral deposits and electrical discharges. Masek & Turcotte (1993) have proposed a modified DLA model for river networks.

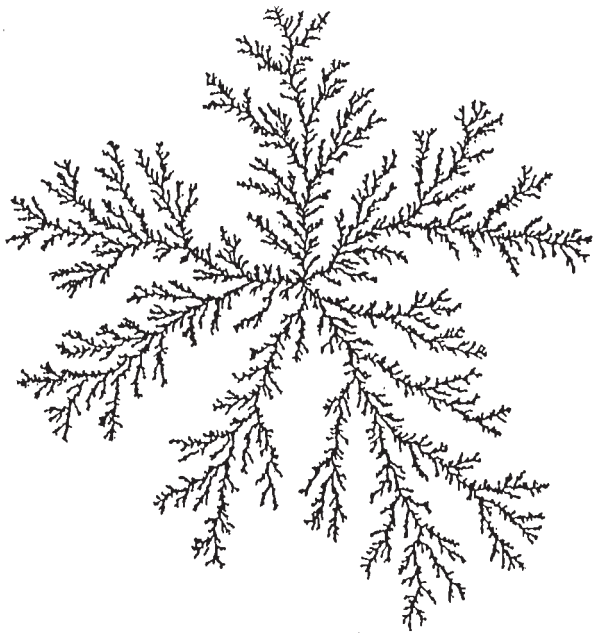

FIG. 10. A two-dimensional, off-lattice DLA cluster with 10^6 particles (Ossadnik, 1992).

5. Vein Structure in a Leaf

We next compare the branching and side-branching statistics of a river network and the vein structure of a leaf. Peckham (1995) developed a software routine for obtaining the statistical properties of river networks from digital elevation models (DEMs). He studied a number of river basins and showed that they exhibit Tokunaga side-branching statistics to a good approximation. One of the basins he considered was the Kentucky River basin, this network is illustrated in Fig. 12(a). This is an eighth-order network that has an area of 13500 km. The branching ratio is $R_N = 4.6$, the length-order ratio is $R_L = 2.5$, and the fractal dimension from (3) is $D = 1.67$. The triangular branching-ratio matrix for this network is given in Fig. 13(a). We now determine values for T_k by averaging the values of $T_{i,i+k}$ over i

$$T_k = \frac{1}{n-k} \sum_{i=1}^{n-k} T_{i,i+k}. \tag{18}$$

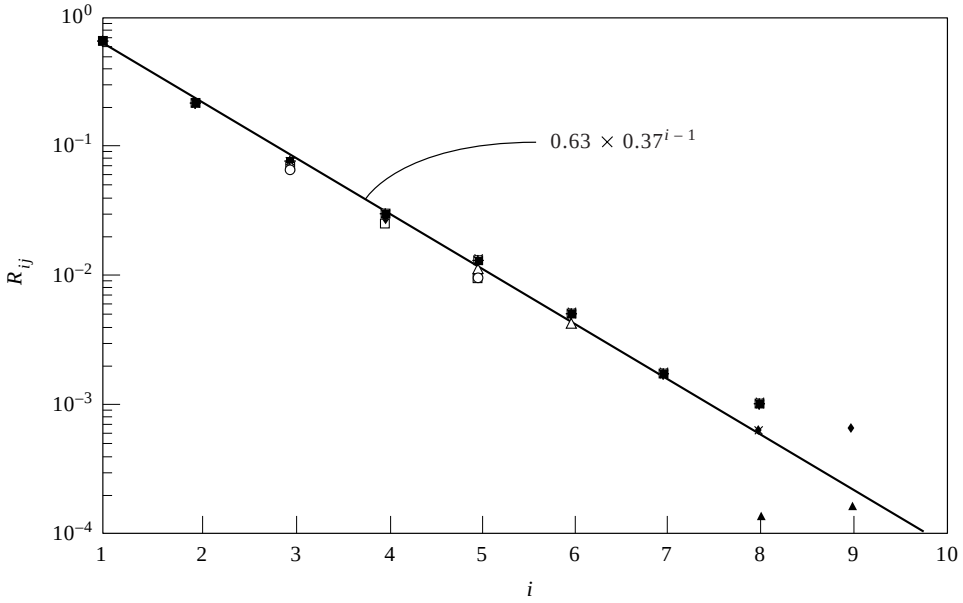

FIG. 11. Dependence of the terms of the ramification matrix R_{ij} for the branching statistics of a diffusion limited aggregation (DLA) cluster on the branch order i for various branch orders j (j: (+) 1; (*) 2; (x) 3; (○) 4; (□) 5; (◇) 6; (△) 7; (■) 8; (♦) 9; (▲) 10). Branches of order i join branches of order j so that $i < j$. The data points are for an average of 47 off-lattice DLA clusters each with 10^6 particles (Ossadnik, 1992). The straight-line correlation is with the Tokunaga relation (17) taking $c = 2.7$.

The values of T_k for the network are given in Fig. 14 as a function of k. It is seen that the results correlate well with (6) taking $a = 1.2$ and $c = 2.5$.

The software routine developed by Peckham (1995) has also been applied in order to obtain the vein structure of leaves. An example is given in Fig. 12(b). This vein structure of a side lobe of a leaf of *Sorbus hybrida* (Rosaceae) was obtained from a grey scale image given by Merrill (1978). The small scale structure of the leaf qualitatively resembles the drainage network illustrated in Fig. 12(a).

The leaf network is ninth order with a branching ratio $R_N = 4.47$, a length-order ratio $R_L = 2.19$, and the corresponding fractal dimension from (3) is $D = 1.91$. The triangular branching-ratio matrix for the leaf lobe is given in Fig. 13(b). The corresponding values of T_k were obtained using (18) and are given as a function of k in Fig. 14. Again there is a generally good correlation with the Tokunaga relation (6) taking $a = 1.2$ and $c = 2.5$. The deviations for $k = 7$ and 8 can be attributed to the smallness of the statistical sample.

6. Allometry

Power-law scaling relations have been recognized in biology and are generally referred to as allometric scaling (Calder, 1984; Schmidt-Nelson, 1984; Niklas, 1994b). An example of allometric scaling is the power-law dependence of the metabolic rate B of an organism on its mass M

$$B \sim M^a \tag{19}$$

The exponent generally takes a value of $a \approx 0.75$. This dependence is illustrated in Fig. 15.

The origin of the scaling given in (19) has been discussed in the literature a great deal. One explanation is based on the structural requirements for elastic support (McMahon, 1973; Miklas, 1994a). Alternative explanations based on fractal tree taxonomies of cardiovascular systems have been given by Barenblatt & Monin (1983) and by West *et al*. (1997). We will consider the approach given by West *et al*. (1997) utilizing the Tokunaga taxonomy.

In obtaining the allometric scaling of metabolic rate and mass a number of assumptions are made:

(1) Fractal scaling

We will assume that our model cardiovascular system obeys the Tokunaga self-similar fractal tree scaling rules introduced in Section 2. This includes the basic order description of branching given in Fig. 1(c). We also assume that the branching satisfies a constant branching ratio as defined in (1) as well as the Tokunaga side branching condition given in (6). The length-order ratio introduced in (2) is also taken to be a constant. We further introduce the area-order ratio

$$R_A = \frac{A_{i+1}}{A_i} \tag{20}$$

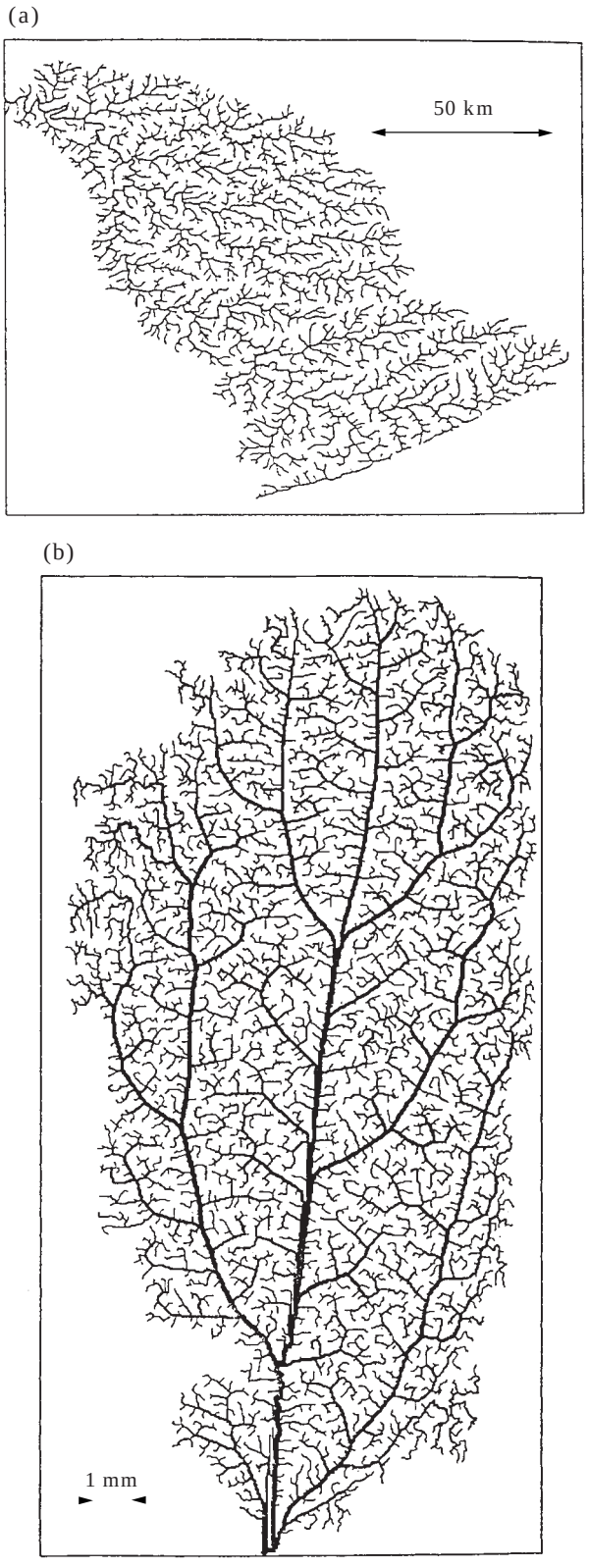

FIG. 12. (a) River network of the Kentucky River basin, Kentucky; (b) vein structure of a side lobe of a mature leaf in *Sorbus hybrida* (Rosaceae) obtained using a scanning routine on a grey scale image given by Merrill (1978).

where A_i is the mean cross-sectional area of branches of order i. We assume that R_A is a constant independent of order, and we take the total order of the cardiovascular system to be n. While the applicability of the assumption for cardiovascular systems is generally accepted, its applicability to bronchial systems has been questioned (West *et al.*, 1986).

(2) Blood volume is proportional to body mass

We assume that blood mass M_{bn} for a mammal with a cardiovascular system of order n is a fixed fraction of the total mass M_n of the mammal

$$M_{bn} \sim M_n \tag{21}$$

assuming blood density is approximately constant across species, (21) is equivalent to

$$M_n \sim V_{bn} \tag{22}$$

where V_{bn} is the volume of blood in a species of order n. This assumption has been justified by West *et al.* (1997) in terms of minimum energy dissipation.

(3) Metabolic rate is proportional to blood flow

It is assumed that the metabolic rate B_n is proportional to the flow of blood Q_n

$$B_n \sim Q_n \tag{23}$$

Different species are able to transport the same metabolism per unit flow of blood.

(4) Smallest order blood vessels are scale independent

It is assumed that the efficiency of transferring nutrients from the smallest order blood vessels to cells is independent of size. If each of the order one branches carries the same blood flow, then the total number of first-order branches N_1 is proportional to the total blood flow Q_n

$$Q_n \sim N_1 \tag{24}$$

The ability of nutrients to diffuse from the smallest branches prescribes a scale to the smallest branches which is independent of the species considered.

(5) Volume filling

The fractal dimensions D of the network is a measure of the extent to which the network is volume filling. If the branching system is fully volume filling we have $D = 3$. In general the branching order and length-order ratios, R_N and R_L, are related from (3) by

$$R_N = R_L^D \tag{25}$$

For a network that comes close to being volume filling we expect D to be slightly less than 3.

1.1	3.2	7.6	15.6	54.8	87.0	408.
	1.1	2.8	6.2	20.3	27.0	115.
		1.2	2.9	10.8	16.0	40.
			1.0	3.2	5.3	20.
				1.8	2.0	12.
					1.0	3.
						1.

(a)

1.67	6.42	14.08	28.06	54.53	114.56	265.0	73
	1.31	3.10	7.67	20.84	63.89	98.5	12
		0.94	1.93	3.29	10.33	29.5	9
			0.88	2.03	6.22	15.5	9
				0.82	2.78	7.0	2
					1.22	4.0	1
						2.0	1
							0

(b)

FIG. 13. Branching ratio matrices for (a) Kentucky River basin illustrated in Fig. 12(a) and (b) for the side lobe of the leaf illustrated in Fig. 12(b).

(6) Branch-area scaling

We assume that the mean area of branch i, A_i, is related to the areas of the lower order branches entering it in such a way that the area to a power α is preserved. Again assuming a binary Tokunaga tree with side branching this condition requires

$$A_1^\alpha = 2A_{i-1}^\alpha + \sum_{j=i-1}^{1} N_{ji}A_j^\alpha = 2A_{i-1}^\alpha + \sum_{k=1}^{i-1} T_k A_{i-k}^\alpha$$

$$= 2A_{i-1}^\alpha + a\sum_{k=1}^{i-1} c^{k-1}A_{i-k}^\alpha \quad (26)$$

in direct analogy to (7). If we divide (26) by A_i^α and introduce the area-order ratio from (20) we obtain

$$1 = \frac{2}{R_A^\alpha} + a\sum_{k=1}^{i-1}\frac{c^{k-1}}{R_A^{\alpha k}} \quad (27)$$

And in analogy with (9) this can be written

$$1 = \frac{2}{R_A^\alpha} + \frac{a}{R_A^\alpha}\left[1 + \frac{c}{R_A^\alpha} + \cdots + \left(\frac{c}{R_A^a}\right)^{i-2}\right] \quad (28)$$

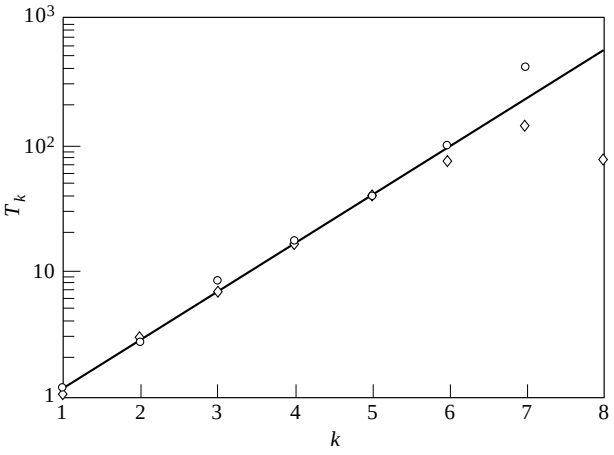

FIG. 14. Dependence of the mean branching ratios T_k on k for the Kentucky River basin illustrated in Fig. 12(a) (○) and for the side lobe of the leaf illustrated in Fig. 12(b) (◇). The straight line correlation is with the Tokunaga relation (6) taking $a = 1.2$ and $c = 2.5$.

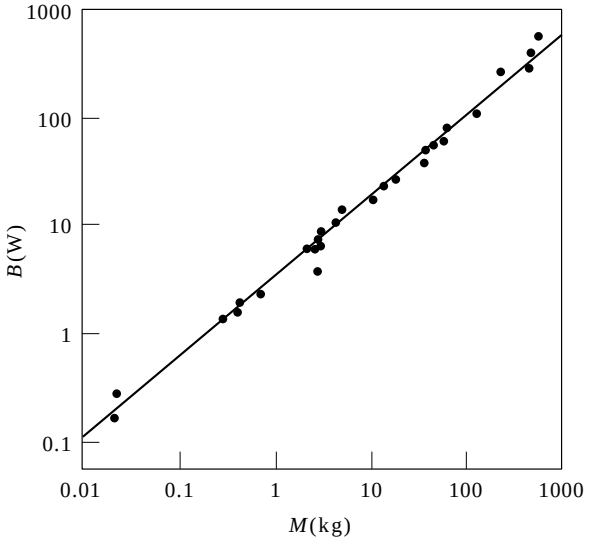

FIG. 15. The dependence of the metabolic rate B on body mass M for a variety of species from mice to elephants (Calder, 1984). The straight-line correlation is from the allometric relation (19) with a $a = 0.75$.

And if $i-2$ is large we can approximate (28) with

$$1 = \frac{2}{R_A^{\alpha}} + \frac{(a/R_A^{\alpha})}{[1-(c/R_A^{\alpha})]} \tag{29}$$

Comparing (8) and (29) we therefore require

$$R_N = R_A^{\alpha} \tag{30}$$

The area order ratio R_A raised to the power α is equal to the branching ratio R_N.

Two branching area laws have been widely proposed for cardiovascular systems. Murray (1926) proposed that $\alpha = 3/2$ on the basis that the laminar viscous impedance is preserved through the network. This is known as Murray's law (Sherman, 1981; La Barbera, 1990). The alternative law is $\alpha = 1$ and area itself is preserved. This has been proposed for the larger arteries on the basis of preserving the acoustic impedance for pulsating flows (Zamir *et al*., 1992; West *et al*., 1997).

We next relate the total blood volume V_{bn} to the branching and length-order ratios. For our self-similar network the total volume of the branches is assumed equal to the blood volume so that we have

$$V_{bn} = \sum_{i=1}^{n} N_i A_i L_i \tag{31}$$

where

$$A_i = A_1 R_A^i \tag{32}$$

$$L_i = L_1 R_L^i \tag{33}$$

$$N_i = R_N^{n-i} \tag{34}$$

Substitution of (32)–(34) into (31) gives

$$V_{bn} = A_1 L_1 \sum_{i=1}^{n} R_N^{n-i} R_A^i R_L^i \tag{35}$$

or

$$V_{bn} = A_1 L_1 (R_A R_L)^n \sum_{i=1}^{n} \left(\frac{R_N}{R_A R_L}\right)^{n-i}$$

$$= A_1 L_1 (R_A R_L)^n \left[1 + \frac{R_N}{R_A R_L} - \cdots \left(\frac{R_N}{R_A R_L}\right)^{n-1}\right] \tag{36}$$

For large values of n with $(R_N/R_A R_L) < 1$ this becomes

$$V_{bn} = \frac{A_1 L_1 (R_A R_L)^n}{1-(R_N/R_A R_L)} \tag{37}$$

Thus we have

$$V_{bn} \sim (R_A R_L)^n \tag{38}$$

And from (22) we obtain

$$M_n \sim (R_A R_L)^n \tag{39}$$

Finally we relate the metabolic rate to the branching ratio R_N. From (24) we require that the blood flow Q_n be proportional to the number of first-order branches N_1. But the number of first-order branches for a self-similar network is given by

$$N_{1n} = \frac{N_1}{N_2}\frac{N_2}{N_3}\cdots\frac{N_{n-1}}{N_n} = R_N^{n-1} \tag{40}$$

We assume n to be sufficiently large that we can approximate this with

$$N_{1n} \sim R_N^n \tag{41}$$

And from (24) we have

$$Q_n \sim R_N^n \tag{42}$$

From (23) we have specified that the metabolic rate B_n is proportion to the blood flow Q_n so that we obtain

$$B_n \sim R_N^n \tag{43}$$

We now have expressions for both quantities in the allometric equation (19).

Substitution of (39) and (43) into (19) gives

$$R_N^n \sim [(R_A R_L)^n]^a = [(R_A R_L)^a]^n \tag{44}$$

or

$$R_N \sim [(R_A R_L)]^a \tag{45}$$

We have previously related R_L to R_N in (25) and R_A to R_N in (30), substituting these two relations into (42) gives

$$R_N \sim (R_N^{1/\alpha} R_N^{1/D})^a = R_N^{a/a} R_N^{a/D} \tag{46}$$

And this can only be satisfied if

$$1 = \frac{a}{\alpha} + \frac{a}{D} \quad \text{or} \quad a = \frac{\alpha D}{D+\alpha} \tag{47}$$

This relation relates the allometric exponent a to the fractal dimension of the cardiovascular system D and the blood-flow resistance parameter α. West *et al*. (1997) argued that $D = 3$ (volume filling) and $\alpha = 1$ (area preserving) with the result that $a = 0.75$ in agreement with the data presented in Fig. 15. The general dependent of a on D $(2 < D < 3)$ for $\alpha = 1$

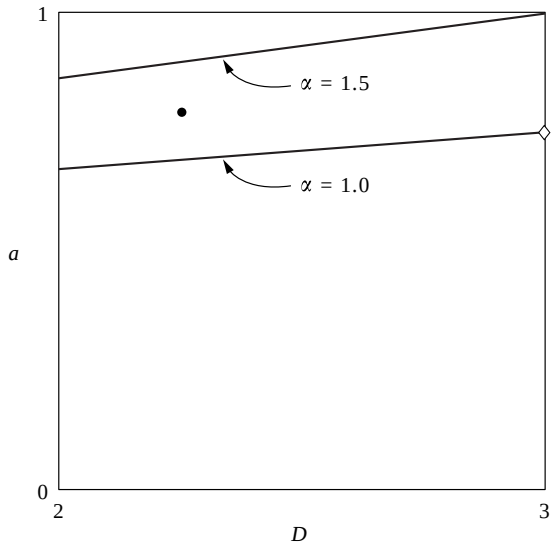

FIG. 16. Dependence of the allometric exponent a on the fractal dimension D for area preserving scaling ($\alpha = 1$) and $A^{3/2}$ scaling ($\alpha = 3/2$) from (47). ($\diamond$) is the result given by West *et al*. (1997) and ($\bullet$) is from the data for the pulmonary arteries of a cat as illustrated in Fig. 17.

and $\alpha = 3/2$ is given in Fig. 16. The allometric exponent falls in the range $2.3 \leqslant a \leqslant 1$.

Morphometric data of the pulmonary arteries of a cat have been given by Fung (1990, p. 205). The branch numbers, branch areas, and branch lengths, were given for the 11-th order network. The data are given in Fig. 17 and excellent fits with the power-law scalings given in (1), (2), and (20) are found. The fits give $R_N = 3.67$, $R_L = 1.78$, and $R_A = 2.92$. From (3) we find that $D = 2.25$ and from (30) we find $\alpha = 1.21$. And from (47) we find that the allometric scaling exponent $a = 0.79$ is close to the value 3/4. This point is also shown in Fig. 16. For this example the fractal dimension $D = 2.25$ is considerably less than volume value $D = 3$ and the blood flow resistance parameter $\alpha = 1.21$ is intermediate between the laminar impedance value $\alpha = 1.5$ and the acoustic impedance value $\alpha = 1$. As shown in Fig. 16 there is a trade-off between the two parameters D and α. If D is somewhat less than 3 and α is somewhat greater than 1 we find that $a \approx 0.75$ is generally a good approximation in agreement with Fig. 15.

7. Discussion

Branching networks play an important role in biology. Examples range from the actual structure of plants and trees to cardiovascular and bronchial systems. The Horton–Strahler taxonomy defining self similarity in terms of number-order and length-order ratios has been found to have wide applicability in biology. The Tokunaga taxonomy extends self similarity to side branching. As a specific example of side branching in biology we consider the vein structure of a leaf. We show that the Tokunaga branching statistics for the leaf are virtually identical to the Tokunaga branching statistics of river

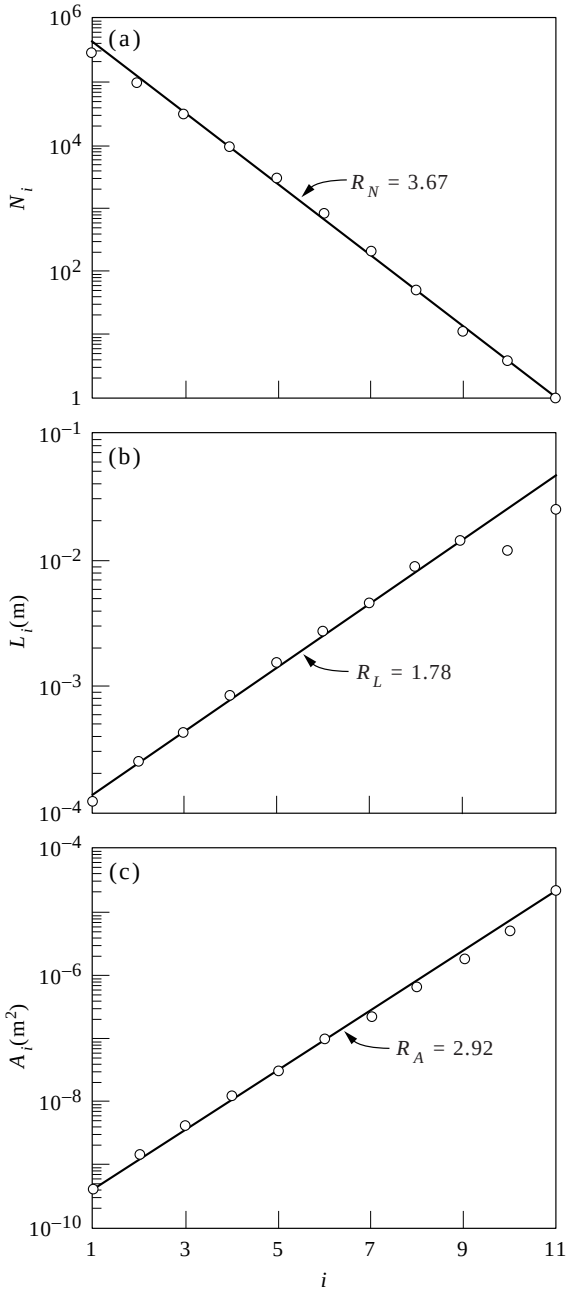

FIG. 17. Morphometric data for the pulmonary arteries of a cat (Fung, 1990, p. 205): (a) branching scaling, number of branches of order i, N_i as a function of order i. The straight-line correlation is from (1) with $R_N = 3.67$; (b) length-order scaling, L_i as a function of i. The straight line correlation is from (2) with $R_L = 1.78$; (c) area-order scaling A_i as a function of i. The straight line correlation is from (20) with $R_A = 2.92$.

networks. It will be of considerable interest to determine whether other networks in biology also exhibit self-similar side branching.

We have shown how self-similar Tokunaga branching networks can be generated both deterministically and stochastically. Using the concept of nodes or buds from which new branches emanate we have constructed space-filling Tokunaga networks in both two and three dimensions. These constructions are highly ordered. As an example of a stochastic Tokunaga network we have considered diffusion limited aggregation (DLA). DLA is a random growth construction that has found a wide range of applications to natural phenomena.

Before addressing the question—why do biological networks exhibit Tokunaga side branching statistics?—we will consider the same question with regard to river networks. A wide variety of models have been proposed to explain the structure of river networks (Rodriguez-Iturbe & Ronaldo, 1997). Many of these models satisfy the self-similarity requirements of constant branching and length-order ratios. However, the required Tokunaga side-branching statistics differentiates between models (Peckham, 1995). The DLA growth model for river networks proposed by Masek & Turcotte (1993) gives Tokunaga side branching with $a = 1.2$ and $c = 2.5$ in agreement with observations (Turcotte, 1997). In this model, random walkers are introduced randomly on a grid. They are allowed to walk until they either intersect with the evolving network or are lost from the grid. The random walkers are viewed as water fluxes that migrate over a relatively flat surface until they find a gully in which to flow. When the flux joins the gully, it erodes and expands the network. An alternate explanation for the structure of river networks is energy minimization. Several authors (Rigon *et al*., 1993; Sinclair & Ball, 1996) have shown that river networks are optimal networks for transporting runoff with the minimum stream power exerted on the landscape. It is clear that at this point in time there is no general agreement on how river networks develop.

We now address the origin of self-similarity of biological networks. Weibel (1991) has argued that fractal geometry is a biological design principal that is most productive; it is an efficient programming of biological forms. Shlesinger & West (1991) argue that fractals are more error tolerant than other structures and therefore have an evolutionary advantage. Biological networks are directly associated with genetic coding so that a stochastic network development is not favored. However, the strong similarities we have illustrated between the vein network in leaves, river networks, and DLA may require a stochastic component to leaf growth.

We finally considered the allometric scaling relation between the metabolic rate and the mass of species in terms of a cardiovascular system with Tokunaga scaling. The approach follows that of West *et al*. (1997). We find that there is a trade-off between the value of the fractal dimension D of the network and the blood flow resistance parameter α. We conclude that value of the allometric scaling exponent a is relatively close to the observed values $a \approx 0.75$ for a range of values of D and α.

We certainly do not consider this paper to be the definitive work on side branching networks in biology. Our purpose has been to introduce the Tokunaga side-branching taxonomy to biology and illustrate its applicability. We hope that our presentation will stimulate further studies in applied areas of biology.

This research has been partially supported under NASA Grant NAGW-4702.

REFERENCES

Barenblatt, G. I. & Monin, A. S. (1983). Similarity principles for the biology of pelgic animals. *Proc. Natl. Acad. Sci. U.S.A.* **80,** 3540–3542.

Barker, S. B., Cumming, G. & Horsfield, K. (1977). Quantitative morphometry of the branching structure of trees. *J. theor. Biol.* **40,** 33–43.

Bassingthwaighte, J. B., Liegovitch, L. S. & West, B. J. (1994). *Fractal Physiology*. Oxford: Oxford University Press.

Calder, W. A. (1984). *Size, Function, and Life History*, 431 pp. Cambridge, MA: Harvard University Press.

Fisher, J. B. & Honda, H. (1979). Branch geometry and effective leaf area: a study of terminalie-branching pattern 1 Theoretical trees. *Am. J. Bot.* **66,** 633–644.

Fung, Y. C. (1990). *Biomechanics*, 569 pp. New York: Springer-Verlag.

Horsfield, K. (1980). Are diameter, length and branching ratios meaningful in the lung? *J. theor. Biol.* **87,** 773–784.

Horsfield, K. (1990). Diameters, generations, and orders of branches in the bronchial tree. *J. Ap. Physiol.* **68,** 457–461.

Horsfield, K., Dart, G., Olson, D. E., Filley, G. F. & Cumming, G. (1971). Models of the human bronchial tree. *J. Apl. Physiol.* **31,** 207–217.

Horton, R. E. (1945). Erosional development of streams and their drainage basins; hydrophysical approach to quantitative morphology. *Geol. Soc. Am. Bull.* **56,** 275–370.

La Barbera, M. (1990). Principles of design of fluid transport systems in zoology. *Science* **249,** 992–1000.

Leopold, L. B. (1971). Trees and streams: the efficiency of branching patterns. *J. theor. Biol.* **31,** 339–354.

Li, K. J. (1996). *Comparative Cardiovascular Dynamics of Mamals*, 156 pp. Boca Raton: CRC Press.

MacDonald, N. (1983). *Trees and Networks in Biological Models*. Chichester: John Wiley.

Mandelbrot, B. (1982). *The Fractal Geometry of Nature*, 460 pp. San Francisco: Freeman.

Masek, J. G. & Turcotte, D. L. (1993). A diffusion limited aggregation model for the evolution of drainage networks. *Earth Planet. Sci. Lett.* **119,** 379–386.

McMahon, T. (1973). Size and shape in biology. *Science* **179,** 1201–1204.

Meakin, P. (1987). The growth of fractal aggregates. In: *Time-Dependent Effects in Disordered Materials* (Pynn, R. & Riste, T., eds), pp. 1–17. New York: Plenum Press.

Meakin, P. (1991). Fractal aggregates in geophysics. *Rev. Geophys.* **29,** 317–354.

Merrill, E. K. (1978). Comparison of mature leaf architecture of three types in Sorbus L. (Rosaceae). *Botan. Gass.* **139,** 447–453.

Murray, C. D. (1926). The physiological principal of minimum work. I—The vascular system and the cost of blood volume. *Proc. Natl. Acad. Sci. U.S.A.* **12,** 207–214.

Nelson, T. R., West, B. J. & Goldberger, A. L. (1990). The fractal lung: universal and species-related scaling patterns. *Experientia* **46,** 251–254.

Newman, W. I., Turcotte, D. L. & Gabrielov, A. M. (1997). Fractal trees with side branching. *Fractals* **5,** 603–614.

Niklas, K. J. (1994a). Size-dependent variations in plant growth rates and the ''3/4-power rule''. *Am. J. Botany* **81,** 134–144.

Niklas, K. J. (1994b). *Plant Allometry*, 395 pp. Chicago, IL: University of Chicago Press.

Ossadnik, P. (1992). Branch order and ramification analysis of large diffusion aggregation clusters. *Phys. Rev.* **A45,** 1058–1066.

Peckham, S. D. (1995). New results for self-similar trees with applications to river networks. *Water Resour. Res.* **31,** 1023–1029.

Rigon, R., Rinaldo, A., Rodriguez-Iturbe, I., Bras, R. L. & Ijjasz-Vasqez, E. (1993). Optimal channel networks: a framework for the study of river basin morphology. *Water Resour. Res.* **29,** 1634–1646.

Rodriguez-Iturbe, I. & Rinaldo, A. (1997). *Fractal River Basins*, 547 pp. Cambridge: Cambridge University Press.

Schmidt-Nielson, K. (1984). *Scaling*, 241 pp. Cambridge: Cambridge University Press.

Sherman, T. F. (1981). On connecting large vessels to small. *J. Gen. Physiol.* **78,** 431–453.

Shlesinger, M. F. & West, B. J. (1991). Complex fractal dimension of the bronchial tree. *Phys. Rev. Lett.* **67,** 2106–2108.

Sinclair, K. & Ball, R. C. (1996). Mechanism for global optimization of river networks from local erosion rules. *Phys. Rev. Lett.* **76,** 3360–3363.

Strahler, A. N. (1957). Quantitative analysis of watershed geomorphology. *Am. Geophys. Un. Trans.* **38,** 913–920.

Tokunaga, E. (1978). Consideration on the composition of drainage networks and their evolution. *Geog. Rep. Tokyo Metro. Univ.* **13,** 1–27.

Tokunaga, E. (1984). Ordering of divide segments and law of divide segment numbers. *Jap. Geomorph. Un.* **5,** 71–77.

Tokunaga, E. (1994). Self-similar natures of drainage basins. In: *Research of Pattern Formation* (Takaki, R., ed.), pp. 445– 468. Tokyo: KTK Scientific Publishers.

Turcotte, D. L. (1997). *Fractals and Chaos in Geology and Geophysics*, 2nd Edn. Cambridge: Cambridge University Press.

Vannimenus, J. & Viennot, X. G. (1989). Combinatorial tool for the analysis of ramified patterns. *J. Stat. Phys.* **54,** 1529–1538.

Weibel, E. R. (1991). Fractal geometry: a design principle for living organisms. *Am. J. Physiol.* **5,** L361–L369.

West, B. J. (1990). Fractal forms in physiology. *Int. J. Mod. Phys.* **B4,** 1629–1669.

West, B. J., Bhargava, V. & Goldberger, A. L. (1986). Beyond the principle of similitude: renormalization in the bronchial tree. *J. Ap. Physiol.* **60,** 1089–1097.

West, G. B., Brown, J. H. & Enquist, B. J. (1997). A general model for the origin of allometric scaling laws in biology. *Science* **276,** 122–126.

Witten, T. A. & Sander, L. M. (1981). Diffusion-limited aggregation, a kinetic critical phenomenon. *Phys. Rev. Lett.* **47,** 1400–1403.

Zamir, M., Sinclair, P. & Wonnacott, T. H. (1992). Relation between diameter and flow in major branches of the arch of the aorta. *J. Biomech.* **25,** 1303–1310.

Zeide, B. & Gresham, C. A. (1991). Fractal dimensions of tree crowns in three lobolly pine plantations of coastal South Carolina. *Can. J. Res.* **21,** 1208–1212.